

# Photocatalytic conversion of cellulose into C5 oligosaccharides.

SKILLEN, N., WELGAMAGE, A., ROBERTSON, P.K.J., IRVINE, J.T.S. and  
LAWTON, L.A.

2023

© 2023 The Author(s). Published by IOP Publishing Ltd. Original content from this work may be used under the terms of the Creative Commons Attribution 4.0 licence. Supplementary materials are appended after the main text of this document.



## PAPER

## Photocatalytic conversion of cellulose into C5 oligosaccharides

## OPEN ACCESS

Nathan Skillen<sup>1</sup>, Aakash Welgamage<sup>2</sup>, Guan Zhang<sup>3,4</sup>, Peter K J Robertson<sup>1,\*</sup> , John T S Irvine<sup>3,\*</sup>  and Linda A Lawton<sup>2,\*</sup>RECEIVED  
28 August 2023REVISED  
15 October 2023ACCEPTED FOR PUBLICATION  
19 October 2023PUBLISHED  
3 November 2023<sup>1</sup> School of Chemistry and Chemical Engineering, Queen's University Belfast, David Keir Building, Stranmillis Road, Belfast BT9 5AG, United Kingdom<sup>2</sup> School of Pharmacy and Life Sciences, Sir Ian Wood Building, Robert Gordon University, Garthdee Road, Aberdeen AB10 7GJ, United Kingdom<sup>3</sup> University of St. Andrews, School of Chemistry, Purdie Building, North Haugh, St Andrews KY16 9ST, United Kingdom<sup>4</sup> School of Civil and Environmental Engineering, Harbin Institute of Technology, Shenzhen (HITSZ), Shenzhen 518055, People's Republic of China

\* Authors to whom any correspondence should be addressed.

E-mail: [p.robertson@qub.ac.uk](mailto:p.robertson@qub.ac.uk), [jtsi@st-andrews.ac.uk](mailto:jtsi@st-andrews.ac.uk) and [l.lawton@rgu.ac.uk](mailto:l.lawton@rgu.ac.uk)**Keywords:** photocatalytic cellulose conversion, sugar production, C5 oligosaccharides, mechanism selectivity, pHSupplementary material for this article is available [online](#)Original content from this work may be used under the terms of the [Creative Commons Attribution 4.0 licence](#).

Any further distribution of this work must maintain attribution to the author(s) and the title of the work, journal citation and DOI.

**Abstract**

Cellulose is made up of linear polymers of glucose monomers that could be a crucial source for valuable chemicals and sustainable liquid fuels. Cellulose is however, very stable and its conversion to a useful fuel or platform chemical products remains a significant challenge (Kimura *et al* 2015 *Sci. Rep.* 5 16266; Xia *et al* 2016 *Nat. Commun.* 7 11162). Photocatalysis is a versatile technology which has demonstrated potential for solar driven processes such as water splitting or solar fuels production and has also been applied to the degradation of pollutants in air and water and for the production of useful products from biomass. Here, we focus on the products that are produced from cellulose (a glucose (C6) based polymer) photocatalysis that compliment hydrogen production. Probing the initial steps *via* UV-TiO<sub>2</sub> photocatalysis, we remarkably find that an array of oligosaccharides containing only five (C5) carbon units is initially produced. As the process continues, C6 oligo oligosaccharides grow to dominate. The photocatalytic process is generally not viewed as a controllable synthetic process; however, these findings show, on the contrary that photocatalysis at semiconductor surfaces can achieve novel reaction pathways yielding new products.

**1. Introduction**

In our search for negative carbon technologies to enable low carbon and net zero economies, the utilisation of solar energy to convert carbon neutral biomass/waste into added value products, is particularly attractive. Cellulose is the most abundant biological macromolecule on earth and is made up of linear polymers of glucose monomers [1]. Due to its high abundance and availability, cellulose could be a crucial source for valuable chemicals and sustainable liquid fuels [1–3]. As a result, there is now increased focus on exploiting cellulose as a major source for green chemistry products, especially for producing sustainable second generation lignocellulose derived liquid fuel [4–6]. Due to its stability, cellulose conversion approaches tend to require high pressure and/or high temperature along with strong acids/bases which pose significant environmental concerns [6–8]. Recent studies have shown that cellulose can be converted into glucose monomers *via* solid acid catalytic approaches such as acid resins, metal oxides, supported metal catalysts and functionalised silicas [9]. The majority of such approaches however, require high temperatures and are best performed under pressure [8].

As an alternative approach, photocatalysis could be applied to cellulose conversion as a cost effective and simple method for harnessing valuable sugars from cellulose biomass, while simultaneously producing hydrogen. Since the initial report on water splitting by Fujishima and Honda [10], photocatalysis has been extensively utilised in environmental remediation applications such as water [11] and air [12] purification

along with systems for H<sub>2</sub> production [13]. Despite the continued growth and expansion of the field, photocatalytic driven cellulose conversion has rarely been reported. There are a number of reports on photocatalysis using cellulose as a sacrificial agent for H<sub>2</sub> production with the initial report by Kawai and Sakata [14] in 1980 and more recently studies utilising Pt-TiO<sub>2</sub> [15, 16] and CdS/CdO<sub>x</sub> photocatalysts for solar lignocellulose conversion [17]. In addition, raw biomass was photocatalytically converted to H<sub>2</sub> by Caravaca *et al* over TiO<sub>2</sub> loaded with a range of precious metals [18]. The formation of H<sub>2</sub> from a sacrificial electron donor (SED) is often the desired product for photocatalytic systems, however the use of expensive or unfavourable SEDs (e.g. oxalic acid [13], acetic acid [19] and alcohols [20]) has often been seen as a limitation. Deploying cellulose as a SED offers an advantage over more traditional compounds due to its abundance and availability in waste materials. Beyond H<sub>2</sub> production however, cellulose also represents a feedstock that can be converted into a range of value-added liquid products, which was partly demonstrated in our previous work by Zhang *et al* [21] and so should strictly not be considered as a ‘sacrificial’ electron donor. Using a composite material of cellulose bound onto TiO<sub>2</sub>, the formation of H<sub>2</sub> was shown along with glucose, cellobiose and formic acid generation in the liquid phase. While this paper, along with others in the field, have highlighted the potential for photocatalytic cellulose conversion, there remains further possibilities for value-added compounds to be generated [22].

Therefore, this study has focused on photocatalytic conversion of cellulose into useful platform chemicals using a composite material that consists of a layer of cellulose surrounding TiO<sub>2</sub> P25. Unlike current cellulose conversion processes, which involve relatively aggressive chemical conditions, the method reported here operates under ambient conditions with minimal power input from four UV lamps (36 W). A very careful series of batch experiments were performed to establish the time dependent evolution of products. Interestingly, the data generated shows the formation of chains of C5 sugar molecules (xylo-oligosaccharides) first as opposed to the expected chains of C6 sugars (hexo-oligosaccharides) that appear in the later stages of the experiments. To date, there has been minimal work focused on photocatalytic conversion of cellulose to non-gas phase products, furthermore, to the best of our knowledge this is the first report showing C5 compounds being generated during the process.

## 2. Experimental

### 2.1. Materials

$\alpha$ -cellulose (Sigma Aldrich) TiO<sub>2</sub> (P25; Evonik), acetonitrile (Sigma Aldrich), trifluoroacetic acid (Fisher Scientific) and ammonium hydroxide (Fisher Scientific) were used as received. Deionised water was supplied from an Elga purification system (18.2 M $\Omega$  cm<sup>-1</sup>, 25 °C).

### 2.2. Cellulose-TiO<sub>2</sub> composite preparation

The composite material of cellulose and TiO<sub>2</sub> (hereafter referred to as cellulose-TiO<sub>2</sub>) was prepared using ball milled cellulose and TiO<sub>2</sub> P25, using methodology previously reported for optimised cellulose/TiO<sub>2</sub> composites for photocatalysis where further details including electron micrographs are presented [21]. Ball milled cellulose (10 g) was prepared by using a Retsch MM 200 mill (Germany) set at 25 Hz (1500 rpm) for 60 mins. To prepare a batch of cellulose-TiO<sub>2</sub>, 1 g of freshly ball milled  $\alpha$ -cellulose and 20 mg of TiO<sub>2</sub> were suspended in 45 ml of water. The suspension was kept in the dark and stirred overnight at room temperature then vacuum dried (40 °C, Genevac) to complete the catalyst immobilisation procedure. Prior to photocatalytic experiments, each individual batch of composite material was washed in 20 ml of water before being centrifuged (4000  $\times$  g, 10 min) and the supernatant removed. The washing step was repeated twice. The supernatant removed was frozen immediately and freeze dried before being reconstituted in 2 ml of water and analysed by UPLC-MS.

XRD characterisation of the freshly prepared cellulose-TiO<sub>2</sub> material was carried out on a PANalytical X'Pert Pro x-ray diffractometer. The x-ray source was copper with a wavelength of 1.5405 Å. All measurements were carried out ex-situ using a spinning stage. The diffractograms were recorded from 5° to 80° with a step size of 0.017°. XRD diffractograms of  $\alpha$ -cellulose and TiO<sub>2</sub> P25 standards along with a cellulose-TiO<sub>2</sub> sample are shown in supplementary figure S1. Previous TEM studies have shown that the TiO<sub>2</sub> nanonparticles were coated with a thin, compact layer of cellulose.

### 2.3. Photocatalytic procedure

In a typical experiment, prewashed cellulose-TiO<sub>2</sub> was suspended into 20 ml water to form the reaction suspension. The pH of this suspension was 6.1 and this was adjusted as required for further studies using trifluoroacetic acid (pH 2 and 4), phosphate (pH 7) and carbonate/bicarbonate buffer tablets (pH 9.6). The reaction suspension was irradiated using a custom light unit composed of four 36 W UV-A compact non-integrated fluorescent lamps [13]. The lamps were positioned to provide 360° irradiation, with the

reaction solution placed in the centre of the lamps at a distance of 6 cm. The lamps had a peak wavelength of 355 nm (supplementary figure S2). The temperature within the light box was maintained at room temperature by a series of built-in fans. The photon flux of the lamps was determined using a potassium ferrioxalate actinometry method [23] and equation (1) below

$$\text{Photon flux} = \frac{\text{Moles of Fe}^{2+}}{\sigma_{\text{Fe}^{2+}} \times t} \quad (1)$$

where ‘moles of  $\text{Fe}^{2+}$ ’ were determined based on the potassium ferrioxalate method, ‘ $\sigma_{\text{Fe}^{2+}}$ ’ was set at 0.97 and ‘ $t$ ’ was the time (min) the actinometry solution was irradiated. The photonic efficiency was then determined based on the calculated photon flux ( $9.2 \times 10^{-6}$  mole of photons  $\text{min}^{-1}$ ) and equation (2)

$$\eta_{\text{photon}} (\%) = \frac{N_e \times \text{Total } N_{\text{sugars}} (\text{moles min}^{-1})}{\text{photon flux (mole of photons min}^{-1})} \times 100 \quad (2)$$

where, ‘ $\eta_{\text{photon}} (\%)$ ’ is the photonic efficiency, ‘ $N_e$ ’ is the minimum number of electrons required to form the sugars, where two electrons are assumed to be involved in each hexose to xylose unit conversion and also for each glycosidic bond splitting. ‘Total  $N_{\text{sugars}}$ ’ is the total rate of sugar formation (either C5 and/or C6) during the illumination period and ‘photon flux’ is the mole of photons entering the reactor per min, as determined by actinometry. The  $\eta_{\text{photon}}$  was calculated for total sugar formation (C5 + C6), C5 only sugar formation and C6 only sugar formation.

Sugar formation rates were determined using a batch-like method of sampling where the reaction suspension was irradiated for a predetermined time before being removed and centrifuged ( $4000 \times g$ , 5 min) to separate the supernatant and cellulose-TiO<sub>2</sub> powder. The entire supernatant was then freeze dried and reconstituted into 2 ml of H<sub>2</sub>O for UPLC-MS analysis. The recovered cellulose-TiO<sub>2</sub> was resuspended in fresh H<sub>2</sub>O and then further irradiated for a predetermined time. In general, the procedure was repeated for irradiation times of 0, 1, 2, 3, 5, 10, 15, 20, 25, 30, 40 and 60 mins with each experiment carried out in duplicate. During irradiation, the reaction suspension was continuously stirred. In addition, control experiments (performed in duplicate) were conducted in the absence of light (dark control), catalyst (light control) and cellulose (sugar control) to confirm that any sugar production was originating from the photocatalytic cellulose conversion.

## 2.4. Analytical methods

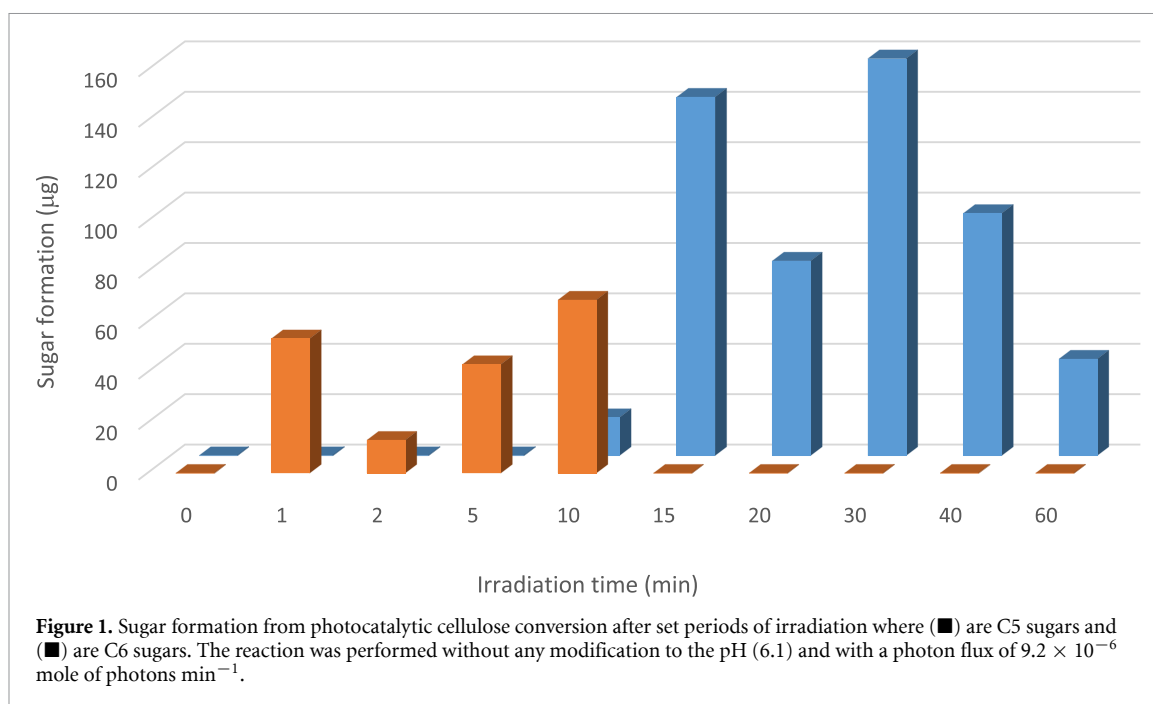
Analysis of the conversion products was performed by an ACQUITY UPLC System with Xevo quadrupole time of flight mass spectrometry in series (Waters, Elstree, UK) using ACQUITY UPLC BEH Amide column (2.1 mm; 100 mm long; 1.7  $\mu\text{m}$  particle size; Waters, UK) maintained at 40 °C. The mobile phase consisted of Buffer A (80% Acetonitrile: 20% Water) and Buffer B (30% Acetonitrile: 70% Water) both containing 0.1% ammonium hydroxide. The separation gradient increased from 0%–60% Buffer B over 10 min at a flow rate of 0.2 ml  $\text{min}^{-1}$  and re-equilibrated for 5 min.

Mass spectrometry (ES-,  $m/z$  50–1500 Da) capillary voltage: 3.0 kV, cone voltage: 25.0 V, source and desolvation temperatures 80 °C and 300 °C respectively. Flow rate for cone gas and desolvation gas: 50 and 400 l  $\text{h}^{-1}$  respectively. To ensure the accuracy of the MS analysis, Leucine enkephalin ( $m/z$  554. 2615 Da) was used as the lock mass reference material at a concentration of 500 pg  $\text{ml}^{-1}$ . The flow rate of the lock mass infusion was set to 10  $\mu\text{l min}^{-1}$  and the lockspray interval was set at 5 s and the data were averaged over 3 scans. Identifications of the C5 and C6 oligosaccharides were based on the retention time and ionised masses compared with commercially available standards (Megazyme, Ireland). For the MS/MS experiments, the collision energy and the cone voltage were adjusted to 45–60 V and 20–30 V respectively. The experiment instrumental control, centroid data acquisition and processing were achieved using Masslynx v4.1.

## 3. Results and discussion

### 3.1. Photocatalytic cellulose conversion

Given that cellulose is a polymer based upon glucose, photocatalytic conversion was expected to release both single monomers and chains of glucose (hexo-oligosaccharides). Interestingly however, upon irradiating the composite cellulose-TiO<sub>2</sub> material, the release of both C5 and C6 oligosaccharides and sugars were detected in the solution phase but with no combined C5 and C6 oligosaccharides being detected (figure 1, supplementary figure S3 and supplementary table S1). Furthermore, it was evident that C5 formation was the dominant process in the first stage of photocatalytic conversion with C5 oligosaccharides being detected after only 1 min of irradiation while C6 formation was only observed after 10 mins. The quantities shown in figure 1 are based on the total C5 or C6 monomer units formed during a given irradiation period, with the

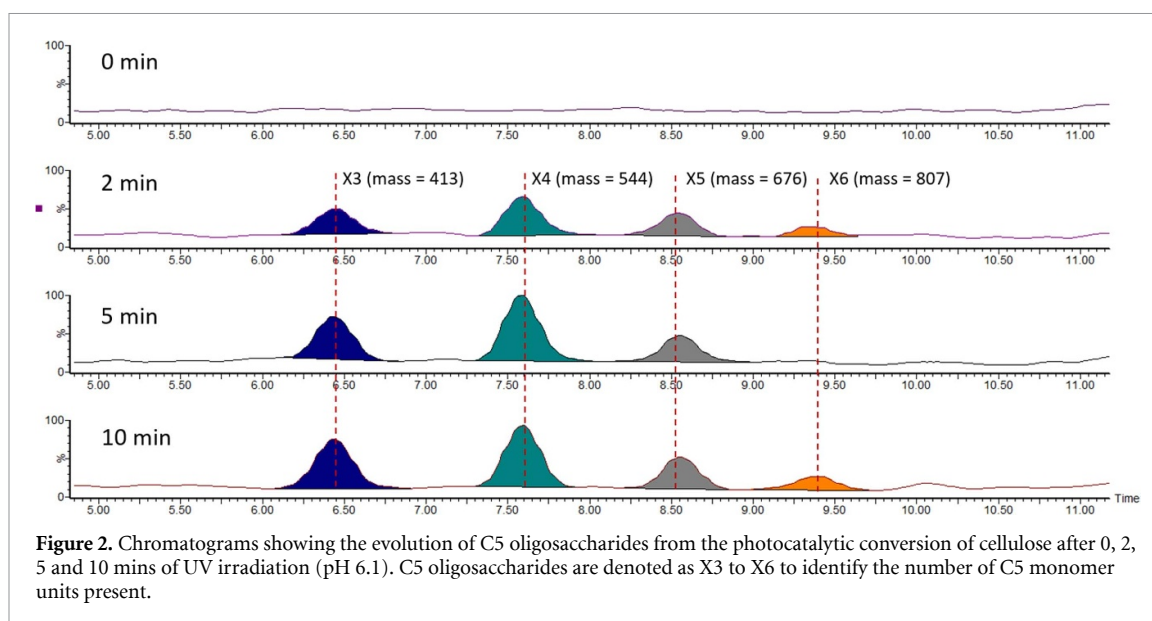


cumulative values reaching 178 and 527  $\mu\text{g}$  for C5 and C6 sugars respectively at 60 min (individual quantities for each sugar are shown in supplementary figure S3 and table S1). To date, the release of C5 sugars from photocatalytic cellulose conversion is yet to be reported, with previous publications detecting only C6 sugars along with additional oxidation products such as formic acid [21]. To confirm that the process reported here was exclusively due to photocatalysis, a series of control experiments were performed. Within all the control experiments (absence of UV light,  $\text{TiO}_2$  and/or cellulose), no sugar formation was detected which confirmed the process was photocatalytic and not a result of photolysis or any pre-treatment stage. Furthermore, UPLC analysis of the starting reaction solution showed no sugars (C5 and/or C6) present. The purity of the  $\alpha$ -cellulose was also confirmed by Raman spectroscopy (supplementary information). It could be purported that C5 sugars resulted from hemicellulose impurities, however, this is highly unlikely since hemicellulose (a branched, cross-linked polymer) is a polymer of a number of different monomers (xylose MW 150.13; galactose MW 180.156; mannose, MW 180.156; rhamnose, MW 164.16, and arabinose, MW 150.13  $\text{g mol}^{-1}$ ). The MS data achieved from the analysis of the photocatalysed cellulose clearly indicates only the presence of chains of xylose monomers (xylo-oligosaccharides). No additional peaks or polymers of alternative masses were found to be present. Further, it is widely reported in the literature [24] that the production of pure xylo-oligosaccharides is complex, typically requiring both chemical and enzymic degradation of selected hemicellulose followed by chromatographic purification.

Analysis of the reaction liquid phase by UPLC-MS, revealed C5 oligosaccharides consisting primarily of 3–6 monomer units along with smaller concentrations of 7 monomer unit chains (figure 2 and supplementary figure S4). The evolution of the C5 oligosaccharides from cellulose in the initial irradiation period is shown in figure 2, highlighting the presence of chains made up of 3–6 monomers (denoted as X3–6). The oligosaccharides were identified by their ionized mass represented in the chromatograms as X3 with a mass to charge ratio of  $m/z$  413  $[\text{M}-2\text{H}]^-$ , X4  $[\text{M}-2\text{H}]^-$  at  $m/z$  544, X5  $[\text{M}-2\text{H}]^-$  at  $m/z$  676 and X6  $[\text{M}-2\text{H}]^-$  at  $m/z$  807. The pentoses arabinose and xylose and the hexoses glucose and galactose and the dihexose cellobiose have been identified in completed photocatalysis experiments as mentioned above and these are likely candidate saccharide components in the oligosaccharide units. Had the xyloses come from trace hemicellulose degradation, mixed C5/C6 oligosaccharides would have been expected, certainly not pure xylose oligosaccharides.

### 3.2. The impact of pH on sugar formation

The release of both C5 and C6 oligosaccharides from the cellulose- $\text{TiO}_2$  suspension suggests the evolving mechanism was complex and potentially dictated by the surface interaction between cellulose and  $\text{TiO}_2$ . In an attempt to reveal the mechanism, the impact of pH was investigated over a range of 2–9.6. It was evident that the formation of C5 and C6 oligosaccharides were influenced by adjusting the pH of the suspension and as a result highlighted a number of key observations (figure 3 and supplementary figure S5). For each pH, the individual quantities of sugars formed are shown while the cumulative values for C5 and C6 sugars from the



time separated batches are presented in the inserts of each graph. The pH clearly impacts not only the quantity of oligosaccharides produced but also the selectivity between C5 and C6 products. The total highest yield of sugar formation (C5 + C6) was detected at pH 4 (1358  $\mu\text{g}$ ) with the remaining dependent on pH in the order of  $9.6 > 6.1 > 7 > 2$  for total amount of sugars formed. In addition to this, the selectivity of C5 sugars was clearly impacted by pH which is highlighted by the ratio of C5 to C6 sugars in the total yield after 1 h at each pH. At pH 2, 19% of the sugars formed were found to be C5 oligosaccharides, with this value increasing significantly to 48% at pH 4. Thereafter, the percentage of C5 sugars present in the total sugar yield decreases with increasing pH with only 4% of the total at pH 9.6 being C5.

The impact of pH on photocatalysis has been well reported and across a range of pathways and mechanisms it has often been shown to influence the surface interaction between the catalyst and substrate [25–27]. While the exact mechanism and its evolution for photocatalytic cellulose conversion is yet to be reported, the authors believe the impact of pH reveals a significant step in the process. The data presented in figure 3 highlighting both the change in sugar formation and the shift in selectivity between C5 and C6 sugars suggests the interaction at the catalyst surface is paramount to the overall efficiency of the system.

### 3.3. Exploring the mechanism of photocatalytic cellulose conversion

While photocatalytic cellulose conversion has become an emerging field of research, the mechanism has not yet been resolved in the published literature, which generally focuses on the final product, rather the evolution of product distribution with time. In  $\text{TiO}_2$  photocatalysis for conversion of organics, it is typically considered that hydroxyl radicals ( $\cdot\text{OH}$ ) are the active agents [28], although a possible direct role for valence band holes should not be excluded, especially for conversion of surface bound cellulose. The non-selective nature of OH radical attack coupled with the broad range of potential oxidative products that can be released, makes determining the pathway challenging. Moreover, both these parameters can be influenced by the often-limited cellulose-catalyst interaction. Therefore, when exploring the photocatalytic mechanism of cellulose conversion into sugars in this study, there were a number of key parameters which were considered; the method of immobilising cellulose onto  $\text{TiO}_2$ , the subsequent catalyst-substrate interaction and the impact of pH on the yield of sugar production. In relation to the formation of the cellulose- $\text{TiO}_2$  composite, this overcame the significant limitations of cellulose insolubility and limited catalyst-substrate surface interaction. Immobilisation of  $\text{TiO}_2$  onto cellulose has previously been reported in relation to hydrogen production [21]; where it was found that ball milling of cellulose before adding the catalyst enhanced  $\text{TiO}_2$  immobilisation by reducing cellulose particle size which increased the binding surface area (per unit mass) for the catalyst. This was achieved on freshly ball milled  $\alpha$ -cellulose, anchoring  $\text{TiO}_2$  onto the hydroxyl groups in the cellulose structure. The ball milled cellulose particles are thought to be grafted to the surface of  $\text{TiO}_2$  by chemisorption and can be described as a two-step procedure involving condensation of surface hydroxyl groups and formation of intra-molecular H-bonds between cellulose strands and  $\text{TiO}_2$  [29, 30]. This approach of anchoring compounds to  $\text{TiO}_2$  has previously been reported and is a result of the

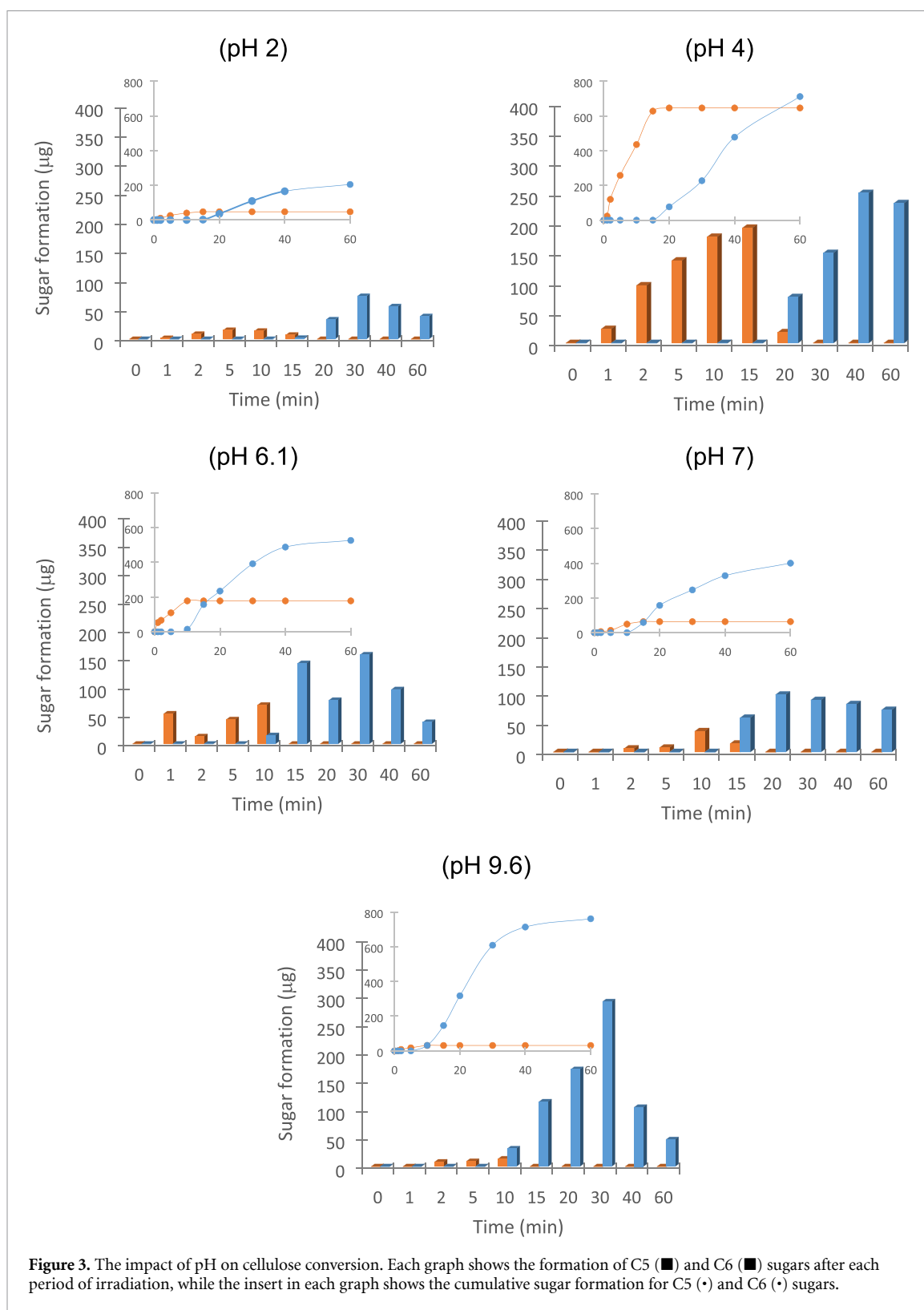
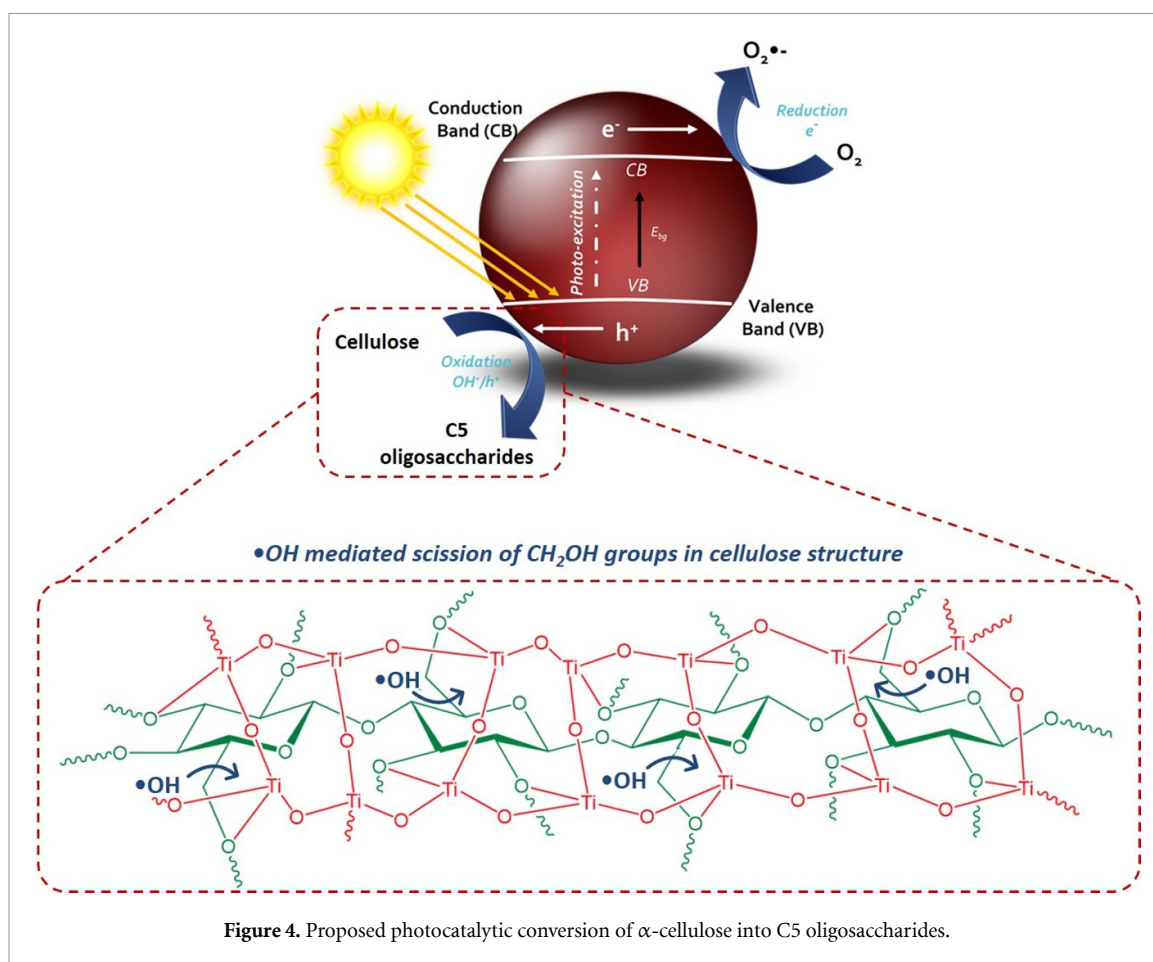


**Figure 3.** The impact of pH on cellulose conversion. Each graph shows the formation of C5 (■) and C6 (■) sugars after each period of irradiation, while the insert in each graph shows the cumulative sugar formation for C5 (•) and C6 (•) sugars.

formation of a ‘Ti-ligand’ between the catalyst surface and compounds that have multiple hydroxyl groups [15]. Moreover, the catalyst seemed to be well attached to the cellulose as it was not removed during the washing procedure prior to photocatalysis.

The binding of cellulose to TiO<sub>2</sub> facilitated an interaction at the surface, which the authors believe played a key role in the formation of C5 sugars. The photocatalytic conversion of cellulose to a series of C5 oligosaccharides rather than C6 products was an intriguing observation in this study and direct conversion by this process has previously never been reported. Previous studies have considered that glucose is the product from cellulose photocatalysis and that this glucose may undergo further conversion, with arabinose



but not xylose being observed in our previous study [21], whilst Hao *et al* report arabinose, galactose, and xylose in their study, attributing these along with formic acid to glucose oxidation [31]. In the current study, the C5 oligosaccharides were formed predominantly during the early stages of photocatalysis, generally within the first 15 mins of UV irradiation, while the formation of C6 oligosaccharides dominated in the later stages of the photocatalytic process (figure 1). As is often reported in photocatalytic processes, the formation and role of the  $\cdot\text{OH}$  typically dictates the reaction pathway. Based on the data presented here, the conversion of cellulose into C5 oligosaccharides seems to occur *via* the  $\cdot\text{OH}$  mediated scission of the hydroxymethyl groups ( $-\text{CH}_2\text{OH}$ ) of cellulose which were bound to the surface of  $\text{TiO}_2$  particles (figure 4). This would mean that the resulting xylose unit in the oligosaccharide was no longer bound to the  $\text{TiO}_2$ , although the adjoining saccharide units should still be bound. Upon further irradiation and subsequent generation of more highly reactive  $\cdot\text{OH}$  species by  $\text{TiO}_2$ , neighbouring hexosaccharide units will undergo further scission of the surface bound  $-\text{CH}_2\text{OH}$  groups, which allows xylose oligosaccharide units to be free to break away from the polysaccharide following scission of the glycosidic linkages, which was probably also a photocatalytic process.

As the photocatalytic process continued beyond 15 min, cellulose conversion into C6 as opposed to C5 oligosaccharides was observed to dominate. Then it appeared that the cellulose which was initially well-bound to the surface of the  $\text{TiO}_2$  has been consumed and now the  $\cdot\text{OH}$  attack on the cellulose molecule occurs away from the surface of the  $\text{TiO}_2$  photocatalyst. In this case, the non-bound cellulose undergoes photocatalytic breakdown into C6 oligosaccharides simply by the scission of the glycosidic bonds that join the glucose monomers in cellulose, as might have been expected from consideration of relative bond strengths in the molecule. This would therefore suggest that conversion to C5 oligosaccharides required the cellulose to be bound to the photocatalyst surface prior to attack by the  $\cdot\text{OH}$ . It is often suggested that the  $\cdot\text{OH}$  generated at the  $\text{TiO}_2$  surface are not selective to specific substrates [17, 21] and furthermore, are capable of diffusing (over a limited range) away from the surface into the bulk solution. Under these conditions, the conversion of cellulose into C6 oligosaccharides is thought to proceed *via*  $\cdot\text{OH}$  mediated cleavage of the glycosidic bonds between glucose monomers and the hydrogen bonding within the cellulose network [30]. The  $\cdot\text{OH}$  mediated decomposition of cellulose to C6 sugars has been previously reported [32].

**Table 1.** Calculated peak formation and photonic efficiency for C5, C6 and total sugar formation across a pH range of 2–9.6.

		pH				
		2	4	6.1	7	9.6
C5 Sugars	Peak formation ( $\mu\text{g}$ )	47.28	646.33	178.32	63.53	31.20
	$\eta_{\text{photon}}$ (%)	1.5	9.8	5.2	1.4	0.9
C6 Sugars	Peak formation ( $\mu\text{g}$ )	204.74	711.04	526.59	400.36	761.04
	$\eta_{\text{photon}}$ (%)	0.3	1.8	1.1	0.6	1.3
Total Sugars	Peak formation ( $\mu\text{g}$ )	252.02	1357.37	704.91	463.89	792.24
	$\eta_{\text{photon}}$ (%)	1.8	11.6	6.3	2.0	2.2

It was proposed that this process was initiated by hydrogen abstraction from the glucose molecules in the structure resulting in the cleavage of glycosidic bonds [32].

It has been previously demonstrated that pH can have a significant effect on the rate of photocatalytic reactions [27, 33, 34]. Moreover, monitoring the impact of pH on photocatalytic reactions can often indicate the mechanism taking place [25]. In this study, adjusting the pH not only impacted the quantity of sugars being formed but also the selectivity between either C5 or C6 oligosaccharide formation. C5 oligosaccharides formation seemed to be favoured at pH 4 (figure 3 and supplementary figure S5). This may be due to a combination of changes in the surface charge of the photocatalyst which influenced adsorption of substrates and potential hydrophobic effects [27, 33, 34]. The point of zero charge for P25 TiO<sub>2</sub> is around 6.25, meaning below this point the photocatalyst has a positive surface charge, while above pH 6.25 it has a negative surface charge [27, 34]. At pH 4 where the TiO<sub>2</sub> has a positive charge, the cellulose-catalyst surface binding affinity appears to be stronger, promoting the binding *via* the –CH<sub>2</sub>OH groups. Tan *et al* carried out zeta potential measurements of microcrystalline cellulose and showed the point of zero charge for the material was 2.8 [34]. Above this pH it had a negative charge which would favour adsorption to the positively charged TiO<sub>2</sub> photocatalyst, thus the pH range where both surfaces favour electrostatic interaction was between 6.25 and 2.8, *i.e.* where the most C5 oligosaccharides were produced. This could therefore account for the higher yields of the C5 oligosaccharides at pH 4 while lower yields were obtained at pH values where the surface adsorption of the TiO<sub>2</sub> to the cellulose would be less favoured due to electrostatic repulsion. At much lower pH, however, there is also the possibility that the higher concentration of protons near the surface of the photocatalyst may undergo reduction by a conduction band electron forming a hydrogen radical. These hydrogen radicals may generate competition as they will readily react with the hydroxyl radicals to form water [26] before they can react with the cellulose. Alternatively, it has been suggested that the pH may also influence the nature of the oxidising species in photocatalytic systems, but this is difficult to accurately determine [29]. Consequently, it appears that at the lower pH values the surface reaction of the cellulose with the TiO<sub>2</sub> photocatalyst was less favoured and hence the yields of both C5 and C6 carbohydrates was lower (figure 3).

### 3.4. Photonic efficiency

As a unit of measurement,  $\eta_{\text{photon}}$  is useful for determining and comparing photocatalytic activity. In this instance, it is used to determine the  $\eta_{\text{photon}}$  for sugar formation based on the peak production of C5 and C6 oligosaccharides individually along with total sugar formation (table 1). The efficiency was calculated as the ratio between moles of sugars produced multiplied by the number of electrons involved and the photon flux of the system ( $0.916 \times 10^{-6}$  mole of photons  $\text{min}^{-1}$ ). It is worth noting that the  $\eta_{\text{photon}}$  shown here may be an underestimation as only the rate of sugar production is taken into consideration. In any photocatalytic system, continuous oxidation can lead to a number of smaller organic compounds forming with complete mineralisation liberating CO<sub>2</sub>, which were not measured in this system. The  $\eta_{\text{photon}}$  values shown in table 1 reflect the results shown in earlier figures, highlighting pH 4 to be optimum for both C5 and C6 oligosaccharide formation. Peak values of 9.8% and 1.8% were obtained at pH 4 for C5 and C6 sugars respectively. Interestingly, while increasing the pH reduced the  $\eta_{\text{photon}}$  for C5 sugar formation, a small increase was seen from pH 7 to 9.6 for C6 sugars. This may be a result of electrostatic repulsion between the TiO<sub>2</sub> and cellulose particles, as discussed, which prevents surface interaction and subsequent formation of C5 sugars, but does allow the diffusion of •OH to break the glycosidic bonds on the cellulose chains.

## 4. Conclusion

Whilst there are several reports of hydrogen production from photocatalytic cellulose conversion, shown here for the first time is the potential of this process to yield high value and novel chemicals such as C5 oligosaccharides. Careful sequential batch studies were performed in order to fully understand the evolution of the process, most notably the products were either C5 or C6 oligosaccharides, but not mixed. The pH studies results indicated that the photocatalytic conversion of cellulose to C5 and C6 oligosaccharides was occurring *via* two distinct mechanisms; one being a cellulose-catalyst surface bound reaction and the other being the breakdown of glycosidic bonds of cellulose away from the surface. During the initial surface bound stage, it appears that photogenerated  $\bullet\text{OH}$  cleaves neighbouring  $-\text{CH}_2\text{OH}$  pendant groups of cellulose polymers. In this stage of the process, C5 selectivity was generally 100%. This ease of  $\bullet\text{OH}$  mediated scission suggests that these groups are coordinated to the  $\text{TiO}_2$  surface under the experimental conditions. In later stages where cellulose was no longer so well bound to  $\text{TiO}_2$ , C6 production dominated. The data also showed pH 4 to be the optimum condition for oligosaccharide formation with total values over 1 h reaching  $1358 \mu\text{g}$  (48% C5) at a photonic efficiency of  $\sim 12\%$ . Overall, the study shown here highlights the potential for photocatalytic cellulose conversion to be controllable and hence to form a range of value-added compounds, which could offer a new negative carbon route to important speciality chemicals.

## Data availability statement

The research data underpinning this publication can be accessed at <https://doi.org/10.17630/6f2acc8f-95ed-47d3-b218-71358b06503e> [35].

## Acknowledgments

The authors thank the Engineering and Physical Sciences Research Council, UK (EPSRC) for funding (EP/K036769/1). Dr Nathan Skillen also thanks the Energy Pioneering Research Program at Queens University Belfast for supporting his research. We also thank Christine Edwards (RGU) for her help on organising the data and preparing the MS data files for the manuscript.

## ORCID iDs

Peter K J Robertson  <https://orcid.org/0000-0002-5217-661X>

John T S Irvine  <https://orcid.org/0000-0002-8394-3359>

## References

- [1] Himmel M E, Ding S, Johnson D K, Adney W S, Nimlos M R, Brady J W and Foust T D 2007 Biomass recalcitrance: engineering plants and enzymes for biofuels production *Science* **315** 804–7
- [2] Sheehan J 2009 Engineering direct conversion of  $\text{CO}_2$  to biofuel *Nat. Biotechnol.* **27** 1128–9
- [3] Kimura M, Shinohara Y, Takizawa J, Ren S, Sagisaka K, Lin Y, Hattori Y and Hinestroza J P 2015 Versatile molding process for tough cellulose hydrogel materials *Sci. Rep.* **5** 16266
- [4] Xia Q, Chen Z, Shao Y, Gong X, Wang H, Liu X, Parker S F, Han X, Yang S and Wang Y 2016 Direct hydrodeoxygenation of raw woody biomass into liquid alkanes *Nat. Commun.* **7** 11162
- [5] Sutton A D, Waldie F D, Wu R, Schlaf M, Silks L A III and Gordon J C 2013 The hydrodeoxygenation of bioderived furans into alkanes *Nat. Chem.* **5** 428–32
- [6] Roman-Leshkov Y, Barrett C J, Liu Z Y and Dumesic J A 2007 Production of dimethylfuran for liquid fuels from biomass-derived carbohydrates *Nature* **447** 982–5
- [7] Sun Y and Cheng J 2002 Hydrolysis of lignocellulosic materials for ethanol production: a review *Bioresour. Technol.* **83** 1–11
- [8] Alonso D M, Bond J Q and Dumesic J A 2010 Catalytic conversion of biomass to biofuels *Green Chem.* **12** 1493–513
- [9] Hu L, Lin L, Wu Z, Zhou S and Liu S 2015 Chemocatalytic hydrolysis of cellulose into glucose over solid acid catalysts *Appl. Catal. B* **174–175** 225–43
- [10] Fujishima A and Honda K 1972 Electrochemical photolysis of water at a semiconductor electrode *Nature* **238** 37–38
- [11] Shannon M A, Bohn P W, Elimelech M, Georgiadis J G, Marinakos B J and Mayes A M 2008 Science and technology for water purification in the coming decades *Nature* **452** 301–10
- [12] Zhao J and Yang X 2003 Photocatalytic oxidation for indoor air purification: a literature review *Build. Environ.* **38** 645–54
- [13] Skillen N, Adams M, McCullagh C, Ryu S Y, Fina F, Hoffmann M R, Irvine J T S and Robertson P K J 2016 The application of a novel fluidised photo reactor under UV–visible and natural solar irradiation in the photocatalytic generation of hydrogen *Chem. Eng. J.* **286** 610–21
- [14] Kawai T and Sakata T 1980 Conversion of carbohydrate into hydrogen fuel by a photocatalytic process *Nature* **286** 474–6
- [15] Zhang G, Kim G and Choi W 2014 Visible light driven photocatalysis mediated via ligand-to-metal charge transfer (LMCT): an alternative approach to solar activation of titania *Energy Environ. Sci.* **7** 954–66
- [16] Chang C, Skillen N, Nagarajan S, Ralphs K, Irvine J T S, Lawton L A and Robertson P K J 2019 Using cellulose polymorphs for enhanced hydrogen production from photocatalytic reforming *Sustain. Energy Fuels* **3** 1971–5

- [17] Wakerley D W, Kuehnel M F, Orchard K L, Ly K H, Rosser T E and Reisner E 2017 Solar-driven reforming of lignocellulose to H<sub>2</sub> with a CdS/CdOx photocatalyst *Nat. Energy* **2** 17021
- [18] Caravaca A, Jones W, Hardacre C and Bowker M 2016 H<sub>2</sub> production by the photocatalytic reforming of cellulose and raw biomass using Ni, Pd, Pt and Au on titania *Proc. R. Soc. A* **472** 20160054
- [19] Zheng X, Wei L, Zhang Z, Jiang Q, Wei Y, Xie B and Wei M 2009 Research on photocatalytic H<sub>2</sub> production from acetic acid solution by Pt/TiO<sub>2</sub> nanoparticles under UV irradiation *Int. J. Hydrog. Energy* **34** 9033–41
- [20] Chen W, Chan A, Sun-Waterhouse D, Llorca J, Idriss H and Waterhouse G I N 2018 Performance comparison of Ni/TiO<sub>2</sub> and Au/TiO<sub>2</sub> photocatalysts for H<sub>2</sub> production in different alcohol-water mixtures *J. Catal.* **367** 27–42
- [21] Zhang G, Ni C, Huang X, Welgamage A, Lawton L A, Robertson P K J and Irvine J T S 2016 Simultaneous cellulose conversion and hydrogen production assisted by cellulose decomposition under UV-light photocatalysis *Chem. Commun.* **52** 1673–6
- [22] Liu X, Duan X, Wei W, Wang S and Ni B J 2019 Photocatalytic conversion of lignocellulosic biomass to valuable products *Green Chem.* **21** 4266–89
- [23] Hatchard C G and Parker C A 1956 A new sensitive chemical actinometer—II. Potassium ferrioxalate as a standard chemical actinometer *Proc. R. Soc. A* **235** 518
- [24] Vázquez M J, Alonso J L, Dominguez H and Parajó J C 2000 Xylooligosaccharides: manufacture and applications *Trends Food Sci. Technol.* **11** 387–93
- [25] Kelly J, Morrison G, Skillen N, Manesiotis P and Robertson P K J 2019 An investigation of the role of pH in the rapid photocatalytic degradation of MCPA and its primary intermediate by low-power UV LED irradiation *Chem. Eng. J.* **359** 112–8
- [26] Alkaim A F, Kandiel T A, Hussein F H, Dillert R and Bahnemann D W 2013 Enhancing the photocatalytic activity of TiO<sub>2</sub> by pH control: a case study for the degradation of EDTA *Catal. Sci. Technol.* **3** 3216–22
- [27] Lawton L A, Robertson P K J, Cornish B J P A, Marr I L and Jaspars M 2003 Processes influencing surface interaction and photocatalytic destruction of microcystins on titanium dioxide photocatalysts *J. Catal.* **213** 109–13
- [28] Hoffmann M R, Martin S T, Choi W and Bahnemann D W 1995 Environmental applications of semiconductor photocatalysis *Chem. Rev.* **95** 69–96
- [29] Chen H and Fu X 2016 Industrial technologies for bioethanol production from lignocellulosic biomass *Renew. Sustain. Energy Rev.* **57** 468–78
- [30] Kim G, Lee S and Choi W 2015 Glucose-TiO<sub>2</sub> charge transfer complex-mediated photocatalysis under visible light *Appl. Catal. B* **162** 463–9
- [31] Hao H, Zhang L, Wang W and Zeng S 2018 Facile modification of titania with Nickel sulfide and sulfate species for the photoreformation of cellulose into hydrogen *ChemSusChem* **11** 2810–7
- [32] Fan H, Li G, Yang F, Yang L and Zhang S 2011 Photodegradation of cellulose under UV light catalysed by TiO<sub>2</sub> *J. Chem. Technol. Biotechnol.* **86** 1107–12
- [33] Kormann C, Bahnemann D W and Hoffmann M R 1991 Photolysis of chloroform and other organic molecules in aqueous titanium dioxide suspensions *Environ. Sci. Technol.* **25** 494–500
- [34] Tan K B, Abdullah A Z, Horri B A and Salamatina B 2016 Adsorption mechanism of microcrystalline cellulose as green adsorbent for the removal of cationic methylene blue dye *J. Chem. Soc. Pak.* **38** 651–64
- [35] Skillen N, Welgamage A, Zhang G, Robertson P K J, Irvine J T S and Lawton L A 2023 *Photocatalytic conversion of cellulose into C5 oligosaccharides*. Dataset University of St Andrews Research Portal (<https://doi.org/10.17630/6f2acc8f-95ed-47d3-b218-71358b06503e>)

## **Photocatalytic conversion of cellulose into C5 oligosaccharides**

Aakash Welgamage<sup>a</sup>, Nathan Skillen<sup>b</sup>, Guan Zhang<sup>c,d</sup>, Peter K. J. Robertson<sup>b\*</sup>, John T. S. Irvine<sup>c\*</sup> and Linda A. Lawton<sup>a\*</sup>

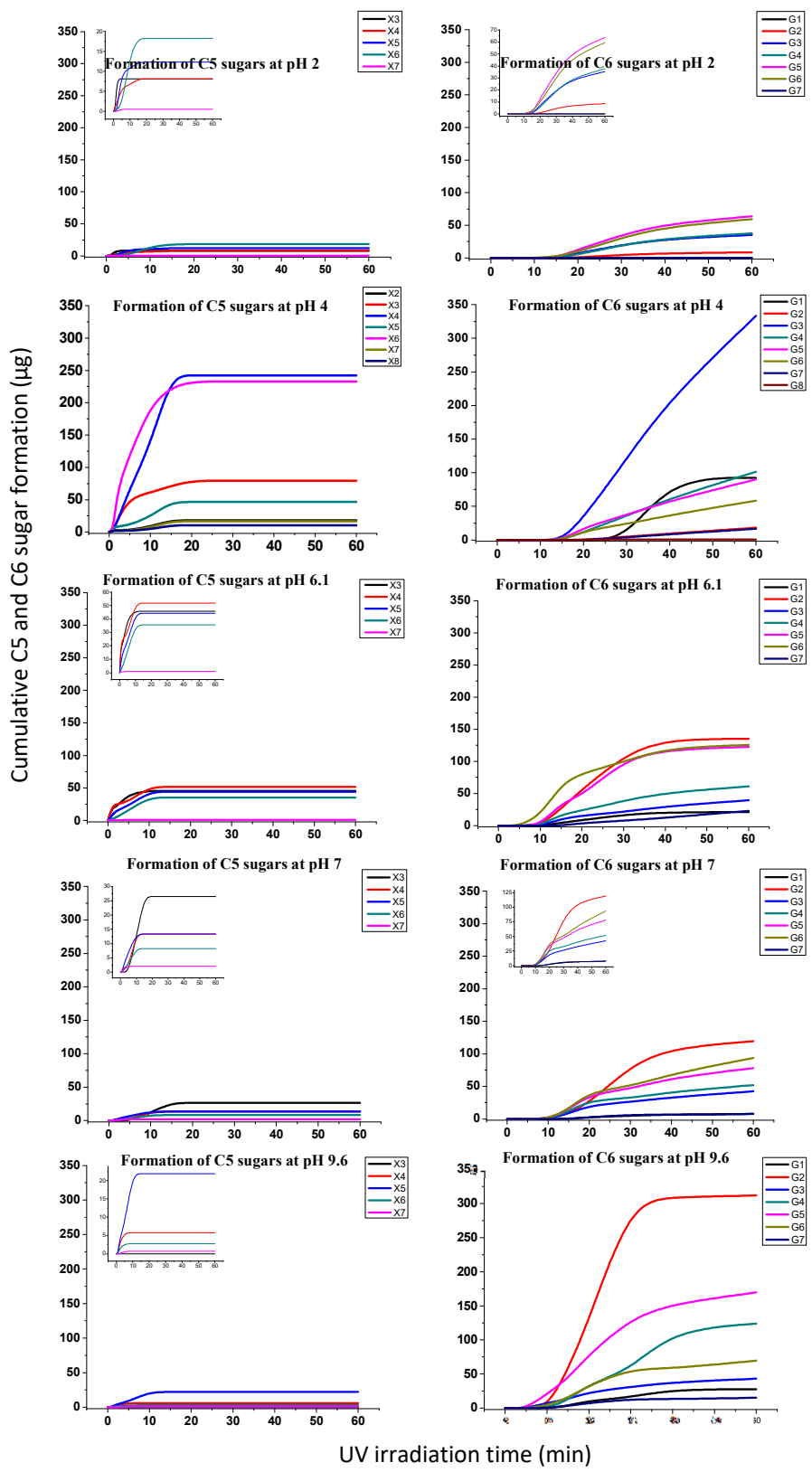
a. School of Pharmacy and Life Sciences, Robert Gordon University, Aberdeen, AB10 7GJ

b. Centre for Energy Sustainability, School of Chemistry and Chemical Engineering, Queen's University Belfast, David Keir Building, Stranmillis Road, Belfast, BT9 5AG.

c. School of Chemistry, University of St Andrews, St Andrews. Fife KY16 9ST

d. School of Civil and Environmental Engineering, Harbin Institute of Technology, Shenzhen (HITSZ), Shenzhen 518055, PR. China

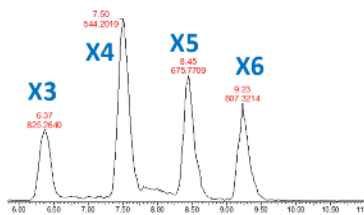
### **Supplementary Information**



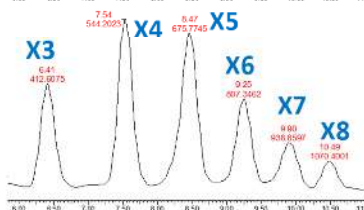
**Supplementary Fig. S1:**  
**Representation of the cumulative formation of C5 and C6 oligosaccharides at different pH during photocatalysis.** C5 and C6 oligosaccharides are denoted with X (xylose) and G (glucose) respectively. For e.g. X3 represents a C5 oligosaccharide with three C5 monomers whereas G3 represents a C6 oligosaccharide with three C6 monomers.

a)

C5 oligosaccharides standard mixture



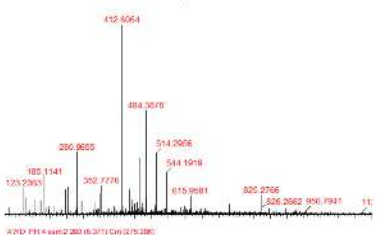
Sugars produced during cellulose photocatalysis



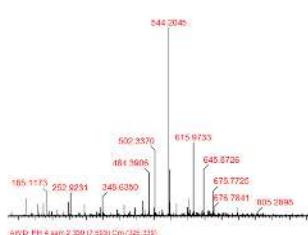
b)



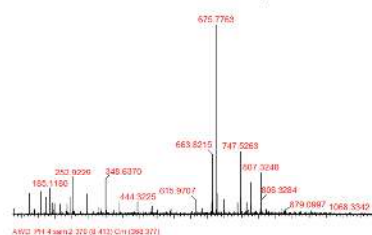
X3 in the sample



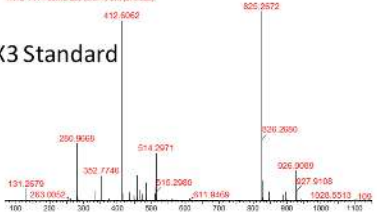
X4 in the sample



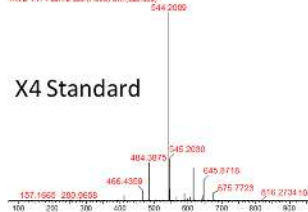
X5 in the sample



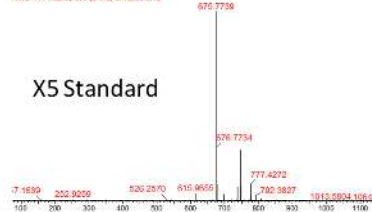
X3 Standard



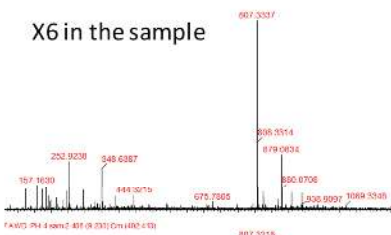
X4 Standard



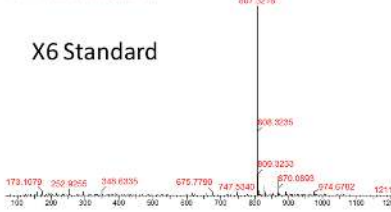
X5 Standard



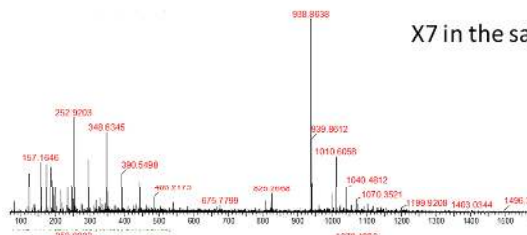
X6 in the sample



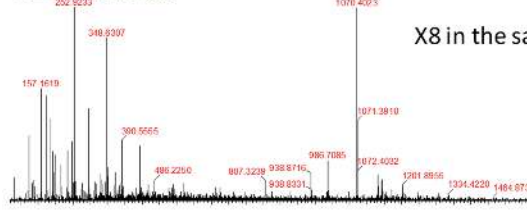
X6 Standard



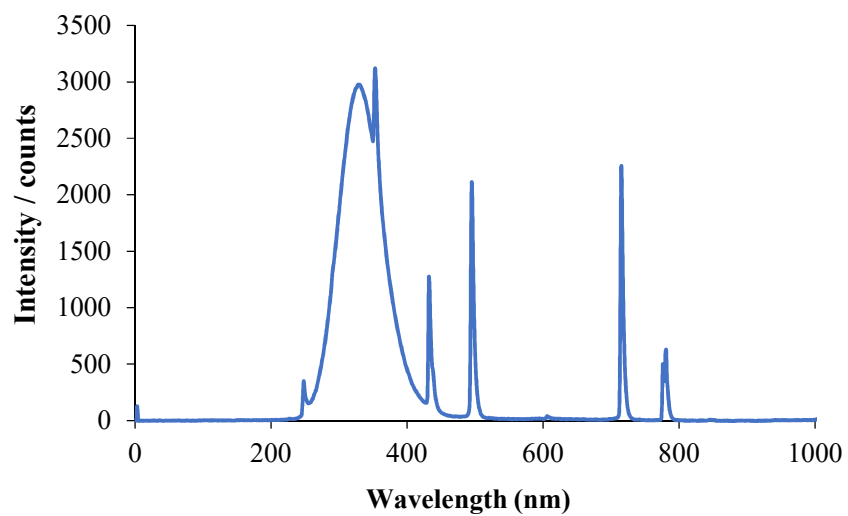
X7 in the sample



X8 in the sample



**Supplementary Fig. S2:** a) UPLC-MS chromatograms of C5 oligosaccharide standards and the C5 oligosaccharides produced during UV photocatalysis of cellulose after 1 min of UV irradiation at pH 4. b) Mass spectra of C5 oligosaccharides produced during photocatalysis and corresponding C5 oligosaccharide standards. X7 and X8 were identified from mass and characteristic fragments as no standards were available.



**Supplementary Fig. S3: Spectral output of 36 W UV-A lamps used for the UV irradiation of the catalysts**